J Electroceram (2010) 25:38–44
DOI 10.1007/s10832-009-9586-7

The effect of TiO_2 and P_2O_5 on densification behavior and properties of Anortite-Diopside glass-ceramic substrates

Vitor M. F. Marques · Dilshat U. Tulyaganov · Govind P. Kothiyal · José M. F. Ferreira

Received: 19 September 2007 / Accepted: 20 July 2009 / Published online: 8 August 2009

Abstract In this work the synthesis of anorthite-diopside glass-ceramics (GCs) was carried out via sintering and crystallization of glass powder compacts in the temperature interval 800°C and 950°C. Glass powder compacts with mean particle size of 2 μm were prepared. The effects of adding TiO_2 and P_2O_5 on the sintering behavior of glass powder compacts and on the properties of resultant glass-ceramics were studied. Mechanical, thermal, chemical and dielectric properties of sintered GCs were investigated with the aim to evaluate the potential of the GCs as substrate materials for microelectronics applications.

Keywords Low co-fired ceramics · Glass-ceramics · Sintering · Crystallization · Anorthite-Diopside · Microstructure · Dielectric properties

V. M. F. Marques · D. U. Tulyaganov · J. M. F. Ferreira (✉)
Department of Ceramics and Glass Engineering,
University of Aveiro, CICECO,
3810-193 Aveiro, Portugal
e-mail: jmf@ua.pt

V. M. F. Marques
Department of Materials, University of Oxford,
OX1 3PH Oxford, United Kingdom

D. U. Tulyaganov
State Committee of Geology and Mineral Resources,
Centre of remote sensing and GIS technologies,
11-A, Shevchenko, str.,
100060 Tashkent, Uzbekistan

G. P. Kothiyal
Technical Physics and Prototype Engineering Division,
Bhabha Atomic Research Centre,
Mumbai 400085, India

1 Introduction

Current progress in telecommunications market has been giving place to an intensive development and miniaturization in microwave systems, which are often applied in high frequency applications, such as computer fields, wireless and Bluetooth. So far, alumina ceramics have been the most widely applied substrates in RF applications mainly due to their relatively low dielectric constant at high frequency, ~9. However, low temperature co-fired ceramic (LTCC) have been recognized as a potential alternative because of its high signal propagation, good reliability, low cost and the possibility of co-firing these substrates with less expensive conductors like Ag and Cu [1–3]. LTCC process is able to produce multilayer structures where cavities and heat sinks can be easily incorporated making easier the microelectronic miniaturization [4, 5].

Anorthite ($CaAl_2Si_2O_8$) based glass ceramics (GCs) have been proposed as an reliable alternative for ceramic substrates mainly because of its lower thermal expansion coefficient (4.5×10^{-6} K^{-1}) and low dielectric constant (6.2 at 1 MHz) [6, 7]. Sintering and crystallization parameters of anorthite-based GCs strongly depend on the composition of parent glass and added nucleating agents [8, 9]. Furthermore the resultant porosity due to insufficient densification can degrade the mechanical properties and increase the dielectric loss [9].

Glasses and glass-ceramics belonging to the anorthite-diopside ($CaAl_2Si_2O_8$-$CaMgSi_2O_6$) system are materials largely used in industrial applications [10, 11] due to the opportunity to introduce cheap and abundant raw materials as glass batch constituents, relatively simple operation conditions during fusion and ceramization coupled with large range of crystalline mixtures between anorthite (An) and diopside (Di). In our earlier study [12] synthesis of

GCs corresponding to the anorthite/diopside (An/Di) weight ratios of 60/40, 50/50 and 45/55 was conducted via sintering and crystallization glass powder compacts in the temperature interval 800°C and 950°C.

The present work aims to investigate effect of TiO_2 and P_2O_5 on densification behaviour and properties of 5 compositions in the Anortite-Diopside system. The starting P_2O_5–containing TiO_2-free An/Di=45/55 glass was denoted as F (Table 1). P_2O_5 was completely substituted by TiO_2 in F1. Compositions F2, F3 and F4 feature constant amount of P_2O_5, while the content of TiO_2 gradually increased from F2 to F4. Mechanical, thermal, chemical and dielectric properties of resultant GCs were investigated in order to improve their overall performance as substrate materials for microelectronic applications.

2 Materials and experimental procedure

Technical grade silicon oxide (purity 99.5%), calcium and magnesium carbonates (>99.5%) along with reactive grade Al_2O_3, CaF_2 and $NH_4H_2PO_4$ were used. According to the batch compositions shown in Table 1, homogeneous mixtures of batches (~100 g), obtained by ball milling, were preheated at 1000°C for 1 h for decarburization. Melting in alumina crucibles was carried out at 1580°C for 90 min in air. Homogeneous and bubble free melts were quenched into cold water to obtain frit materials. The frits were subsequently dried at 100°C for 2 h and then milled in a high-speed porcelain mill for 4 h in absolute ethanol, using a 250 mL jar, 10 and 20 mm diameter alumina balls, and a balls to charge ratio of 3:1.

Rectangular bars ($4\times5\times50$ mm^3) and cylindrical pellets (17 mm in diameter and 2 mm in thickness) were obtained by uniaxial pressing (80 MPa) from the fine glass-powders featuring mean particle size of 2 μm. The samples were subjected in heat treatment at 800–950°C (heating rate of 5 K/min; soaking for 1 h at the sintering temperatures).

The following characterization techniques were used. The particle size distribution of the powders was determined by light scattering technique (Coulter LS 230, UK, Fraunhofer optical model). Differential thermal analysis (DTA) was performed in air at a heating rate of 5 K/min (Setaram Labsys TG-DTA/DSC, France). The coefficient of thermal expansion (CTE) of the sintered samples was measured by dilatometry (Bahr Thermo Analyze DIL 801 L, Germany) at a heating rate of 5 K/min. Identification of crystalline phases and determination of their lattice parameters were carried out by X-ray diffraction technique (XRD, Rigaku Geigerflex D/Mac, C Series, Cu K_a radiation, Japan). Microstructure observation (SEM, Hitachi S-4100, Japan, 25kV acceleration voltage) was carried out at polished and then etched glass-ceramic surfaces obtained by immersion in 2 vol.% HF solution for 10 s.

The values of apparent density and porosity were evaluated by Archimedes method (i.e. immersion in ethylenoglycol). Water absorption was measured according to the ISO-standard 10545-3, 1995 (i.e. weight gain of samples after immersion into boiling water for 2 h).

The linear shrinkage upon sintering was calculated from the dimensions of the green and of the sintered samples. The evaluation of mechanical properties comprised measurements of Vickers microhardness (Shimadzu microhardness tester type M, Japan, load of 1.96 N), each point being the mean value of 50 indentations made on 5 different samples (10 measurements in each sample); and three-point bending strength of rectified parallelepiped bars ($3\times4\times50$ mm^3) of sintered GCs (Shimadzu Autograph AG 25 TA, 0.5 mm/min displacement; each value is the mean of 12 measurements). The chemical resistance was evaluated by immersion of prismatic samples ($22.5\times4.5\times4.0$ mm^3) into solutions of 5% NaOH, and 5% HCl at 95°C for 24 h.

Real (ε′) and imaginary (ε′′) permittivity parts were measured in the frequency range of 500 MHz to 3 GHz using the parallel plate resonator method. Samples having dimensions of $7.2\times5.8\times0.25$ mm were placed in the centre of the highest waveguide walls parallel to electrical field.

Table 1 Nominal compositions of different batches (wt.%)*.

Composition	SiO_2	Al_2O_3	CaO	MgO	P_2O_5	CaF_2	TiO_2
F	47.57	15.69	24.60	9.75	2.02	0.37	–
F1	47.57	15.69	24.60	9.75	–	0.37	2.02
F2	47.57	15.69	24.60	9.75	2.02	0.37	2.02
F3	47.57	15.69	24.60	9.75	2.02	0.37	4.00
F4	47.57	15.69	24.60	9.75	2.02	0.37	8.00

*The F GC composition corresponds to the anorthite/diopside (An/Di) weight ratios of An/Di=45/55. In F1, P_2O_5 was replaced by TiO_2. In the compositions F2-F4 the nucleating agent TiO_2 was added in excess to the starting composition F. Therefore, the total wt.% in these compositions exceeds 100

The dissipation loss factor (tanδ) was evaluated using the relation:

$$\mathrm{Tang}\,\delta = \varepsilon''/\varepsilon' \quad (1)$$

Breakdown strength measurements were carried out using an A-10 Udeyraj-Mumbai system. All samples were submitted to an increasing DC current with constant rate of 2.5 kV/s. Measurements were performed in silicon oil using the cylindrical samples.

3 Results and discussion

TiO_2 affected the glass transition temperature (T_g) and the crystallization temperature peak (T_c) as evidenced by the DTA curves (Fig. 1). Particularly, glass F exhibited T_g at 715°C and T_{c1} at 920°C. Another shallow exothermic effect denoting a second crystallization event was detected at the high temperature region. Compared to the starting composition F, in the glass F1, T_g and T_{c1} decreased to 705°C and 895°C, respectively. Moreover, a second crystallization peak having T_{c2}=962°C clearly appeared in DTA curve. Similar results demonstrating a shift of T_g and T_c to lower temperatures region with increasing TiO_2 content were reported for the GCs in the $CaO\text{-}Al_2O_3\text{-}SiO_2$ system [13, 14]. The simultaneous presence of P_2O_5 + TiO_2 in composition F2 led to a decreasing intensity of the first crystallization peak and an increasing intensity of the second one. With further increase of TiO_2 content in compositions F3 and F4, the two crystallization peaks tend to merge into a single one.

The appearance of two crystallization peaks in DTA curves with addition of TiO_2 (compositions F1 and F2) suggests that liquid phase separation might be playing a key role in both nucleation and crystallization processes.

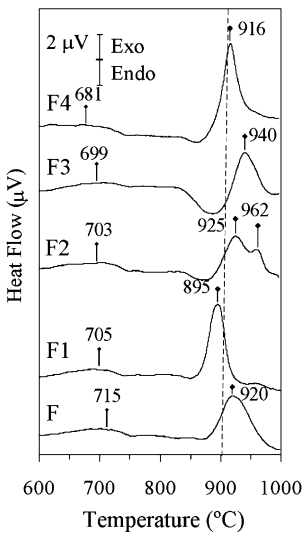

Fig. 1 DTA curves of the glass powders

Formation of anorthite and diopside should occur almost simultaneously in F3 and F4 because they show single exothermic crystallization peaks (Fig. 1). According to Leonelli et al. [10], this can be an indirect indication of the small difference between the activation energies of formation for the two crystals.

Widening of T_c-T_g temperature interval in the starting TiO_2-free composition (F) delayed the crystallization and enhanced the densification process. On the contrary, this interval was reduced in F1, i.e., when P_2O_5 was completely substituted by TiO_2. Earlier studies have reported that P_2O_5 can impart excellent sintering ability increasing stability of the glass against crystallization at the temperature of sintering onset [15, 16]. The effect of P_2O_5 on delaying crystallization was seemingly depressed in F2, F3 and F4 due to presence of TiO_2, which might facilitate phase separation in liquid phase and reduce the activation energy for crystallization [17, 18]. From the Table 2 it can be seen that the addition of TiO_2 caused also a reduction CTE values of experimental GCs.

Figure 2 presents the XRD patterns of sintered GCs. Anorthite and diopside along with traces of akermanite and fluroapatite were revealed in all experimental compositions. Total replacement of P_2O_5 by TiO_2 or the further increasing the added amount of TiO_2 did not result in formation of new phases. XRD patterns of GC F1 exhibited higher crystallinity and an increase in diopside/anorthite ratio compared to GC F suggesting growing of diopside yield with addition of TiO_2. Furthermore, addition of TiO_2 caused a shift in positioning of diopside peaks toward lower 2θ values, which can be associated with growing of diopside's lattice parameters and unit cell volume, as confirmed by the XRD data (not shown). These observations suggest that the substitution of Si^{4+} (ionic radius of 0.40 Å) by Ti^{4+} (ionic radius of 0.56 Å) in the tetrahedral sites of diopside structure has occurred, which is in good agreement with results reported by Birgit et al. [19]. Consequently, a binary solid solution in the range $CaMgSi_2O_6\text{-}CaMgTiSiO_6$ can be formed in GCs F1, F2, F3 and F4.

Figure 3(a) and (b) show the evolution of density and shrinkage, and of water absorption of the samples sintered in the temperature range of 800°C–950°C, respectively. The replacement of P_2O_5 by TiO_2 (GC F1) did not cause noticeable changes in density. In general, the density values of compositions F and F1 remained essentially constant within the whole sintering temperature range. In contrast, GCs F2, F3 and F4 exhibit maximum density values at 800°C that clearly decay with increasing temperature, suggesting that further addition of TiO_2 enhances the porosity of the specimens. Changes in density values are reasonably correlated with the variations registered in shrinkage and water absorption.

Table 2 Coefficients of thermal expansion (CTE) of the glass-ceramics (GC) sintered at 900°C, calculated from the slope of the linear parts of the dilatometry curves between 100°C and 500°C.

Temperature (°C)	CTE ($10^{-6}K^{-1}$)				
	F	F1	F2	F3	F4
100–400	6.79	6.51	6.44	6.04	5.62
100–500	7.15	6.85	6.76	6.36	6.09

The SEM micrographs shown in Fig. 4 illustrate typical microstructures after sintering at 900°C. In the microstructure of GC F (Fig. 4(a)), the composition of which is close to the eutectic composition in the binary anorthite–diopside (An42-D58), two characteristic fields can be distinguished comprising (A) fine relatively coarse crystals (about 3 μm) and (B) with less than 1 μm in length. Composition F1 has a dense microstructure (Fig. 4(b)) with features similar to those observed in composition F. SEM images of compositions F2, F3, and F4, (Fig. 4(c), (d) and (e)) indicate a gradual increase of porosity with increasing contents of TiO_2. On the other hand, Fig. 1, shows that TiO_2 makes T_g to decrease. This suggests that TiO_2 probably favors the formation of less viscous glasses at temperatures close to

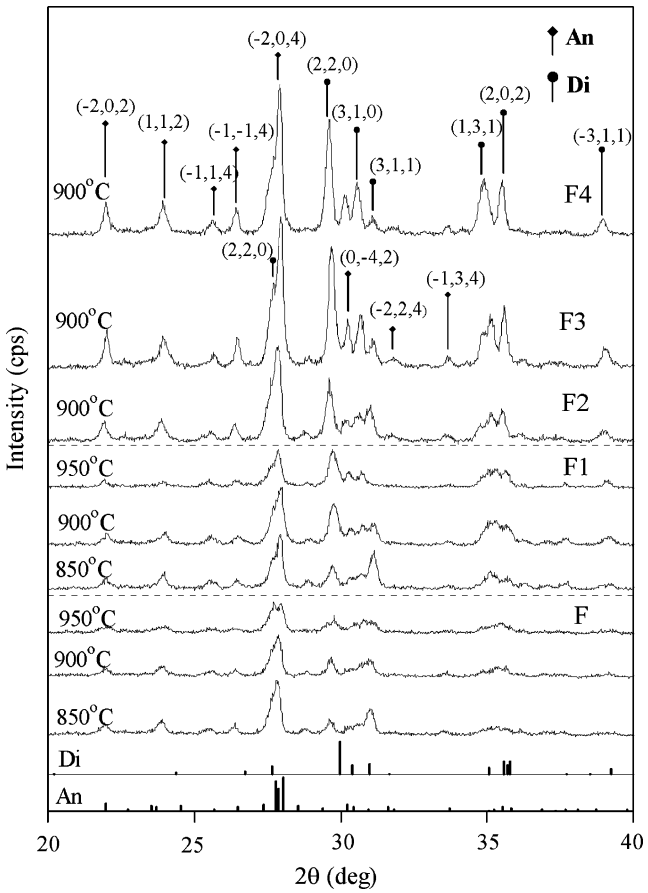

Fig. 2 XRD patterns of the GCs sintered at different temperatures

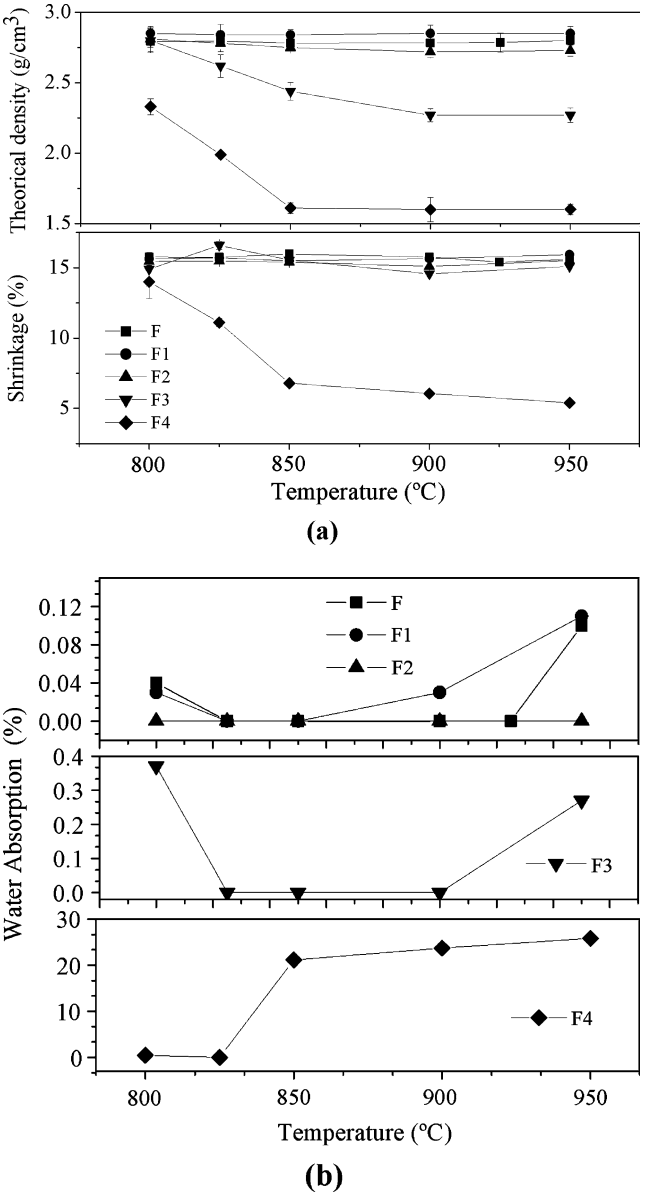

Fig. 3 Properties of the sintered GC compacts and its dependence on the composition and the heat treatment temperature: (**a**) density and shrinkage; (**b**) water absorption

but above T_g, which, in turn, will be more prone to entrapment the gases present in the interstices of frit particles leading the glass matrix to expand and to the formation of large pores, as observed. However, due to its active nucleating role, the viscosity of the melt is expected to increase fast with temperature increasing due to the nucleation and crystallization phenomena, hindering further densification and "frozen" the porous structure formed under the internal pressure of entrapped gases. TiO_2 does not only increases the crystalline fractions of An and Di but also affects the microstructure, which is a quite important factor deciding the thermo-physical properties of glass-ceramics in general. These observations are in close

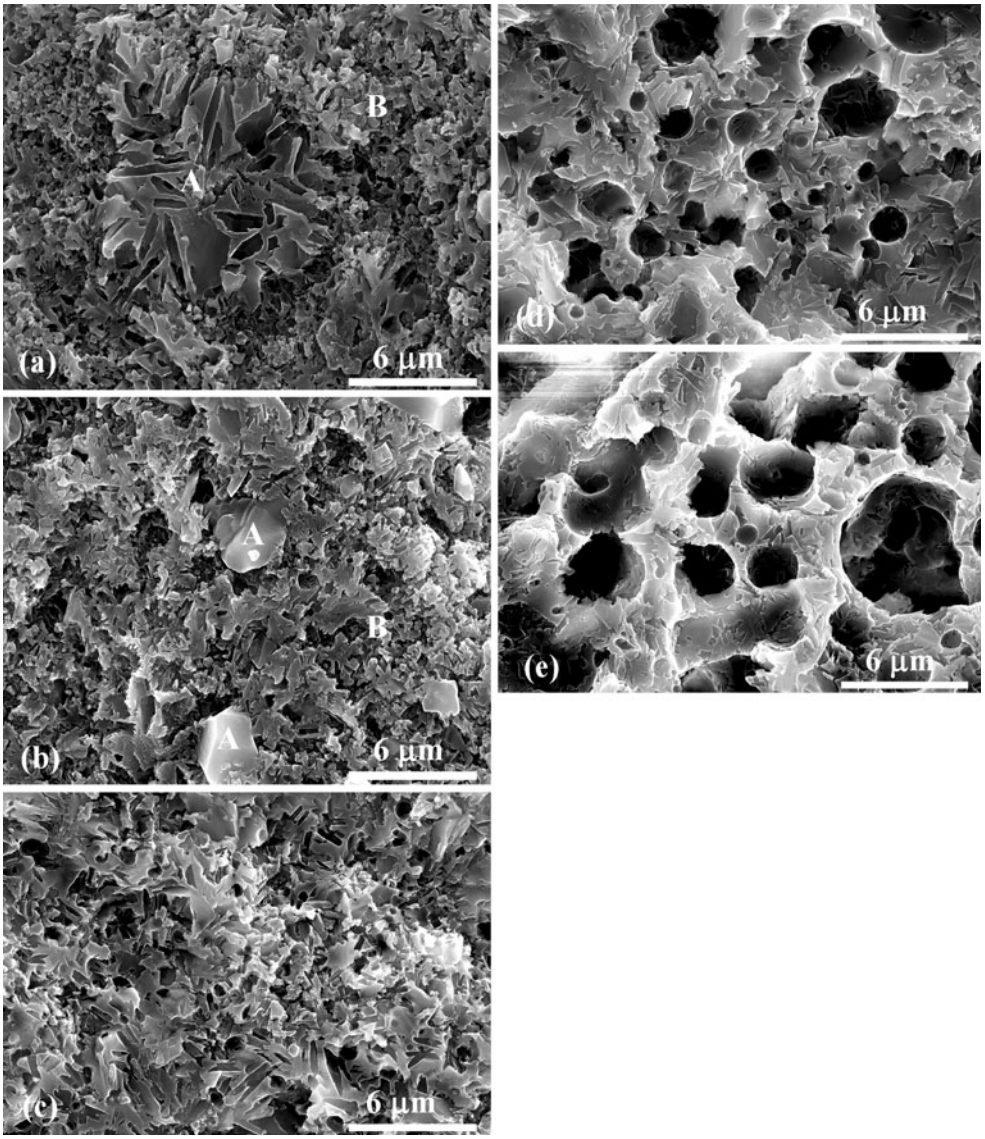

Fig. 4 SEM images of fracture surfaces of GC samples after heat treatment at 900°C (**a**), F; (**b**), F1; (**c**), F2; (**d**), F3; (**e**), F4

agreement with the results presented in Fig. 3. As a matter of fact, the spherical pores shown in the micrographs (d) and (e) of Fig. 4 are typically derived from coalescence of smaller pores, while gases trapped in those pores are responsible for the expansion of the samples. This behavior is well correlated with DTA results that demonstrated a decrease of the temperature interval T_c-T_g responsible for densification with increasing contents of TiO_2.

The results of bending strength are shown in Fig. 5. After sintering at 800°C all experimental compositions (except GC F) exhibited similar flexural strength, what is in good agreement with the values revealed for density. At elevated temperatures the best properties were recorded for GCs F and F2. The latter one featured highest mechanical strength at 950°C. Increasing the TiO_2 content in GCs F3 and F4 deteriorate the mechanical properties due to the appearance of large pores clearly observed in the micrographs (d) and (e) of Fig. 4 (Table 3).

Table 4 shows the results of microhardness and chemical resistance of the investigated GCs after sintering at 900°C. Normally microhardness and CTE change in opposite manner. However, here they show similar trends (F1-F4).

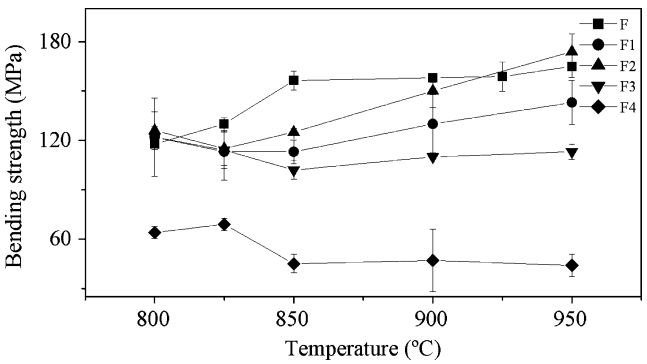

Fig. 5 Dependence of bending strength of sintered GCs on the composition and the heat treatment temperature

Table 3 Semi-quantification phase analysis by XRD, estimated theoretical density, and measured density data of GCs sintered at 900°C.

900°C					
Composition	Phase volume fraction		TD (g cm^{-3})	Measured density	
	An	Di	(estimated)*	(g cm^{-3})	%DT
F	0.78	0.22	2.86	2.78	97.16
F1	0.64	0.36	2.93	2.85	97.42
F2	0.64	0.36	2.93	2.72	92.97
F3	0.59	0.41	2.95	2.27	76.99
F4	0.68	0.32	2.91	–	–

*The theoretical density (TD) was estimated assuming that the samples sintered at 900°C consist exclusively of crystalline phases. Although microstructures shown in Fig. 3 suggest that this might be an acceptable assumption, one should keep in mind that the phase analysis is only semi-quantitative and some remaining glassy should exist among the crystals

This suggests that the microhardness values have been negatively affected by the microstructural features observed in Fig. 4. The data of chemical resistance summarized in Table 4 reveal that the investigated GCs are more chemically resistant in alkaline media than in acidic environment. This is not surprising since GCs are usually more sensitive to acidic environments, particularly those based on Anorthite, (Anorthite is extremely vulnerable to HCl in comparison to Diopside). A semi-quantitative phase analyses gave the following ratios An/Di: 78/22 (F); 64/36 (F1, F2); 59/41 (F3) and 68/32 (F4).

The results of dielectric properties of the samples sintered at 900°C measured at room temperature in the range of 500 MHz to 3 GHz are summarized in Table 5, while Fig. 6 reports the real permittivity part (ε′) and loss tangent (Tang δ=ε′′ /ε′) for GCs sintered at 900°C of the same samples. The results demonstrated that the dielectric constant values of all compositions are low, being situated in the range between 4 and 7. This suggests that addition of TiO_2 (ε′~100) did not promoted significant changes in permittivity, in accordance with the XRD data from which no crystalline phase

Table 4 Microhardness and chemical resistance of GCs sintered at 900°C.

Compositions	Microhardness $HV_{0.2}$ (kgf.mm^{-2})	NaOH loss of mass (μg/cm^2)	HCl
F	558±17	0.535	25.5
F1	610±14	0.557	14.5
F2	530±19	0.469	19.1
F3	325±11	0.011	28.3
F4	88±12	12.8	24.7

Table 5 Room temperature permittivity of glass-ceramic compositions sintered at 900°C.

Composition	ε′ 1.2GHz	Tanδ 1.2GHz	Dielectric Strength (kV/cm)
F	5.1	0.014	158
F1	6.2	0.00017	183
F2	7.2	0.0057	143
F3	4.1	0.0035	140

containing TiO_2 has been identified. On the other hand, the replacement of P_2O_5 by TiO_2 (composition F1) extremely decreased the loss tangent factor at 1.2 GHz from 1.4×10^{-2} to 1.7×10^{-4}, which demonstrates the potential of composition F1 for LTCC applications. Loss tangent values of ~10^{-4} in the range of 0.5 to 2 GHz, the typical Bluetooth band where Al_2O_3 is characterized by a loss tangent of 4×10^{-4} and a permittivity of ~9. The highest and lowest loss tangent values were measured for the compositions F and F1, with P_2O_5 or TiO_2 alone, respectively. In the presence of both nucleating agents, loss tangent decreases with increasing contents of TiO_2, masking the negative effect of P_2O_5 on this property, while increasing the porosity. Therefore, in the compositions F2-F4, the results of loss tangent will be a compromise between the positive and the negative effects of TiO_2.

Regarding to the dielectric strength measurements it was observed that higher densities yielded higher dielectric strengths may be because of the prevention of local electric fields formation. Herein is supposed that glassy phase plays a role as a source of free ionic carriers. This might explain why GC F that is less crystalline than GC F1 also exhibits a lower value of dielectric strength. Furthermore, local electrical fields can be created across weak spots (pores and voids) leading to breakdown failure. Therefore, we feel that F2 and F3 show the lowest dielectric strength values among

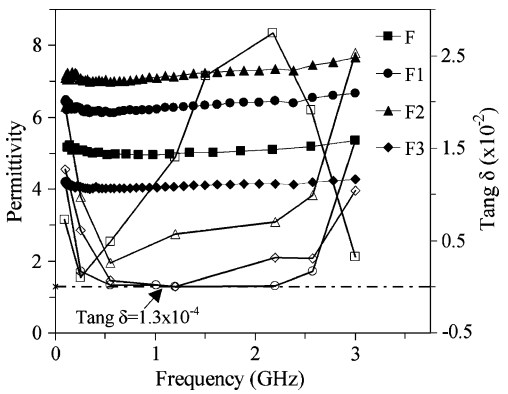

Fig. 6 Real permittivity part (ε′) and loss tangent (Tang δ=ε′′/ε′) for GCs sintered at 900°C

all compositions mainly due to their higher porosity rather than to chemical differences.

4 Conclusions

The results presented and discussed along this work enable the following conclusions to be drawn:

1. P_2O_5 in starting composition F enabled to extend temperature interval T_c-T_g delaying crystallization, being useful for completion of densification.
2. The replacement of P_2O_5 by the same amount of TiO_2 did not cause noticeable changes in density while accelerated the nucleation and crystallization processes;
3. The assemblage of crystalline phases formed in the experimental compositions was always the same, irrespective of the presence of P_2O_5 or TiO_2.
4. The formation of diopside was favored and the overall crystallinity was enhanced in the presence of TiO_2. Increasing added amounts of TiO_2 increased the lattice parameters and unit cell volume of diopside, shifting its XRD peaks to lower 2 theta values, while reduced the CTE of GCs;
5. Density, microhardness, flexural strength, chemical resistance, of the GCs were generally improved in the presence of about 2 wt.% of TiO_2 while higher amounts tend to hinder densification, originate large pores and deteriorate the overall properties of the GCs;
6. The replacement of P_2O_5 by TiO_2 induced a decrease in the loss tangent factor at 1.2 GHz of two orders of magnitude demonstrating the potential of composition F1 for LTCC applications;
7. The dielectric strength was mostly dependent on the sample density. The absence of pores and voids (GC F1) prevent space charge formation and yield higher dielectric strength.

Acknowledgements This study was supported by CICECO and the Portuguese Foundation for Science and Technology (FCT).

References

1. J. Cava, Dielectric materials for application in microwave communications. J. Mater. Chem. **11**, 54–62 (2001)
2. K. Niwa, N. Kamehara, H. Yokoyama, and K. Kurihara, Multilayer ceramic circuit board with copper conductor, in *American Ceramic Society, Westerville,* ed. by J.B. Blum, W.R. Cannon advances in ceramics, vol.19, Multilayer ceramic devices, (OH, 1986), pp.41–48
3. G. Chen, X. Liu, Fabrication, characterization and sintering of glass-ceramics for low–temperature co-fired ceramic substrates. J. Mater. Electr. **15**, 595–600 (2004)
4. J.-W. Sheen, LTCC-MLC Duplexer for DCS-1800. IEEE MTT-Transactions **47**(9), 1883–1889 (1999)
5. Y.-J. Choi, Middle-permittivity LTCC dielectric compositions with adjustable temperature coefficient. Mat. Letters. **58**, 3102–3106 (2004)
6. A. Mergen, Low-temperature fabrication of anorthite ceramics from kaolinite and calcium carbonate with boron oxide addition. Ceram. Int. **29**, 667–660 (2003)
7. V.M.F. Marques, D.U. Tulyaganov, S. Agathopoulos, V.K. Gataullin, G.P. Kothiyal, J.M.F. Ferreira, Low temperature synthesis of anorthite based glass-ceramics via sintering and crystallization of glass-powder compacts. J. Eur. Ceram. Soc. **26**, 2503–2510 (2006)
8. C.-L. Lo, Microstructure characteristics for anorthite composite glass with nucleating agents of TiO_2 under non- isothermal crystallization. Mat. Res. Bul. **37**, 1949–1960 (2002)
9. C.-L. Lo, low temperature sintering and microwave dielectric properties of anorthite-based glass ceramics. J. Am. Ceram. Soc. **85**, 2230–2235 (2002)
10. C. Leonelli, T. Manfredini, M. Paganelli, P. Pozzi, G.C. Pellacani, Crystallization of some anorthite-diopside glass precursors. J. Mater. Sci. **26**, 5041–5046 (1991)
11. L. Barbieri, A.B. Corradi, I. Lancellotti, C. Leonelli, M. Montorsi, Experimental and computer simulation study of glasses belonging to diopside-anorthite system. J. Non-Cryst. Sol. **345–346**, 724–729 (2004)
12. V.M.F. Marques, D.U. Tulyaganov, S. Agathopoulos, J.M.F Ferreira, Low temperature production of glass ceramics in the anorthite–diopside system via sintering and crystallization of glass powder compacts. Ceram. Int. In Press (2007).
13. R.G. Duan, Effect of changing TiO_2 content on structure and crystallization of CaO-MgO-SiO_2 systems glasses. J. Eur. Ceram. Soc. **18**, 1729–1735 (1998)
14. M. Rezvani, Effect of Cr_2O_3, Fe_2O_3 and TiO_2 nucleants on the crystallization of SiO_2-Al_2O_3-CaO-MgO(R_2O) glass ceramic. Ceram. Int. **31**, 75–80 (2005)
15. D.U. Tulyaganov, S. Agathopoulos, H.R. Fernandes, J.M.F. Ferreira, Processing of glass-ceramics in the SiO2-Al2O3–B2O3-MgO-CaO-Na2O-(P2O5)-F system via sintering and crystallization of glass powder compacts. Ceram. Int. **32**, 195–200 (2006)
16. D.M. Miller, Sintered cordierite glass-ceramic bodies, *US Patent 3.926.648 29* May (1976).
17. N. M. Pavlushkin, Principals of glass ceramics technology, 2nd ed., Stroiizdat, Moscow, 1979 (in Russian).
18. Z. Strnad, *Glass-ceramic materials* (Elsevier, Amsterdam, 1986)
19. B. Sepp, The stability of clinopyroxene in the system CaO-MgO-SiO_2-TiO_2 (CMST). Am. Mineral. **86**, 265–270 (2001)